控制与决策
Control and Decision

基于自适应视距制导的无人潜航器三维协同路径跟踪控制

王浩亮, 于德智, 卢丽宇, 张卫东, 彭周华

基于自适应视距制导的无人潜航器三维协同路径跟踪控制

王浩亮[1,2,3,4], 于德智[1,3], 卢丽宇[3,5], 张卫东[2,6], 彭周华[3,4,5†]

(1. 大连海事大学 轮机工程学院，辽宁 大连 116026；2. 上海交通大学 电子信息与电气工程学院，上海 200240；3. 大连市智能船艇集群控制与电气技术重点实验室，辽宁 大连 116026；4. 水路交通控制全国重点实验室，辽宁 大连 116026；5. 大连海事大学 船舶电气工程学院，辽宁 大连 116026；6. 海南大学 信息与通信工程学院，海口 570228)

摘　要: 针对跟踪路径复杂、立体空间运动、模型参数动态变化、风浪流扰动下的多无人潜航器 (unmanned underwater vehicle, UUV) 协同路径跟踪问题开展研究. 首先, 针对UUV跟踪复杂路径情形设计自适应前视距离策略, 使得UUV可以更好地跟踪复杂水下路径; 其次, 针对立体空间运动的UUV集群, 设计三维视距制导律和协同控制律引导UUV集群在三维空间中沿参数化路径运动; 最后, 针对模型参数动态变化、风浪流扰动影响下的UUV集群, 设计自抗扰控制器实现对动态变化模型、总扰动信息和速度信息的统一估计, 保证动力学控制的稳定性. 仿真结果验证了所提出基于自适应视距制导的无人潜航器三维协同路径跟踪控制方法的有效性.

关键词: 自适应前视距离；三维视距制导；协同路径跟踪；自抗扰控制；无人潜航器

中图分类号: U676.1　　**文献标志码:** A

DOI: 10.13195/j.kzyjc.2024.0350

引用格式: 王浩亮, 于德智, 卢丽宇, 等. 基于自适应视距制导的无人潜航器三维协同路径跟踪控 [J]. 控制与决策, 2025, 40(1): 242-251.

Three-dimensional cooperative path following control of unmanned underwater vehicles based on adaptive line of sight guidance

WANG Hao-liang[1,2,3,4], *YU De-zhi*[1,3], *LU Li-yu*[3,5], *ZHANG Wei-dong*[2,6], *PENG Zhou-hua*[3,4,5†]

(1. Marine Engineering College，Dalian Maritime University，Dalian 116026，China；2. School of Electronics, Information and Electrical Engineering，Shanghai Jiao Tong University，Shanghai 200240，China；3. Dalian Key Laboratory of Swarm Control and Electrical Technology for Intelligent Ships，Dalian 116026，China；4. State Key Laboratory of Maritime Technology and Safety，Dalian 116026，China；5. Marine Electrical Engineering College，Dalian Maritime University，Dalian 116026，China；6. School of Information and Communication Engineering，Hainan University，Haikou 570228，China)

Abstract: This paper investigates a cooperative path following problem of multiple unmanned underwater vehicles (UUVs) with complex tracking paths, three-dimensional spatial motion, dynamic changes of model parameters, and wind, wave and current perturbations. Firstly, considering the complexity of tracking paths, an adaptive look forward distance strategy is designed to enable UUVs to better track complex paths. Secondly, for the multiple UUVs moving in three-dimensional space, a line of sight guidance law and a cooperative control law are designed to guide the UUVs to move along the parameterised paths in three-dimensional space. Thirdly, for the UUVs under the influence of dynamic changes in model parameters and disturbances such as wind, waves, and currents, an anti-disturbance controller is designed to achieve a unified estimation of dynamic model variations, total disturbance information, and velocity information, ensuring the stability of dynamic control. Simulation results verify the effectiveness of the proposed three-dimensional cooperative path following control method for the UUVs based on the adaptive line of sight guidance.

Keywords: adaptive look forward distance；three-dimensional line of sight guidance；cooperative path following；anti-disturbance control；unmanned underwater vehicle

---

收稿日期: 2024-04-01；**录用日期:** 2024-08-06.

基金项目: 新一代人工智能国家科技重大专项项目(2022ZD0119902)；国家自然科学基金项目(52071044)；辽宁省自然科学基金项目(博士科研启动计划)(2023-BS-077)；中国博士后科学基金项目(2024M751980)；大连市基础重大项目(2023JJ11CG008)；水路交通控制全国重点实验室开放课题(SKLMTA-DMU2024Y3)；大连海事大学博联科研基金项目/中央高校基本科研业务费专项资金项目(3132023616).

责任编委: 闫敬.

†通讯作者. E-mail: zhpeng@dlmu.edu.cn.

0 引 言

近年来,随着海洋开发的迅猛发展,无人潜航器(Unmanned underwater vehicle, UUV)被广泛应用于科研、商业和军事领域. 多UUV以集群形式协同作业可大大提高其执行复杂海上任务的综合能力,成为未来近海岸与深远海移动作业的重要技术手段,也是UUV的必然发展趋势[1-3].

运动控制技术是UUV完成作业任务的关键技术. 根据协同控制目标的不同,UUV运动控制可分为协同目标跟踪[4-5]、协同轨迹跟踪[6-7]、协同路径跟踪3类. 与前两者相比,协同路径跟踪没有严格的时间限制,只需要在一定误差范围内跟踪期望的路径,若短时间内通信效果不佳或通信链路中断,则各航行器仍可沿预设路径航行以保障安全,通信恢复后可重新进行编队协同,更适合用UUV以集群形式执行作业任务[8-9]. 可用于路径跟踪控制的制导方法主要有纯追踪法[10]、平行接近法[11]和视距(line of sight, LOS)制导策略[12-14]. 文献[10]针对水下航行器的逆流干扰问题,将纯追踪制导与非线性制导相结合实现了路径跟踪控制. 文献[11]提出一种基于平行接近法的自适应滑模路径跟踪控制器,提高了航行器的制导精度. 然而,相对于以上两种制导方法,LOS制导由于具有简单高效、抗干扰能力强、易于实现等优点,被广泛应用于海洋航行器的路径跟踪控制中[15-17]. 文献[15]提出了基于LOS制导律和非线性协同控制律的交叉跟踪控制方法,保持设计队形并跟踪直线路径. 文献[16]设计了基于事件触发的LOS制导策略,有效减轻了无人艇远程控制的网络通信负担. 文献[17]将前视角引入无人艇路径跟踪控制器,通过对输出的视距角进行补偿,提高了LOS制导策略的适应性.

目前,基于LOS制导的路径跟踪控制方法大多适用于二维水平面[15-17]或纵平面[18-19],无法满足UUV执行水下立体空间作业任务的客观需求. 相比于二维平面,三维空间的协同制导需要考虑的因素更多,控制器设计也更具挑战性. 同时,现有LOS制导策略大都采用固定前视距离,当路径复杂且需执行高精度跟踪任务时,需要动态调整前视距离以保证跟踪效果. 然而,传统定视距LOS制导自适应能力差、变视距LOS制导[20]动态响应慢等不足在一定程度上限制了UUV的实际应用.

目前针对海洋航行器的动力学控制方法主要包括PID控制[21]、滑模控制[22-23]、神经网络控制[24-25]、自适应控制[26]、模糊控制[27]和抗干扰控制[28-29]等. 对于UUV而言,其模型参数需要通过大量实验测得,且航行速度、航行器载荷、深水压力等因素都将使得UUV的模型参数动态变化,再加上海风、波浪、洋流等外界干扰,无疑进一步增加了UUV的控制难度. 自抗扰技术由于结构简单、整定方便、鲁棒性好、适用于非线性系统等优势[30],满足UUV这种快机动、大范围、高海况作业的航行器控制需求. 然而,目前采用自抗扰技术对三维空间航行的UUV进行研究的文献相对较少.

本文针对跟踪路径复杂、立体空间运动、模型参数动态变化、风浪流扰动下的多UUV协同路径跟踪问题开展研究. 考虑UUV跟踪路径复杂情形,设计自适应前视距离策略,使得UUV可以更好地跟踪复杂水下路径. 针对立体空间运动的UUV集群,设计三维LOS制导律和协同控制律引导UUV集群在三维空间中沿参数化路径运动. 针对模型参数动态变化、风浪流扰动影响下的UUV集群,设计自抗扰控制器实现对动态变化模型、总扰动信息和速度信息的统一估计,保证动力学控制的稳定性.

与现有海洋航行器协同路径跟踪控制相比,所提出基于自适应视距(adaptive line of sight, ALOS)制导的抗干扰协同路径跟踪控制方法具有如下特点: 与文献[15-17]采用的定视距和文献[20]采用的变视距不同,所提出ALOS制导策略对复杂路径适应能力强、动态响应快. 与文献[15-19]采用的LOS制导仅适用于二维水平面或纵平面相比,所提出三维ALOS制导律可以引导UUV在水下立体空间运动. 与文献[24-26]需要持续激励以实现对动态变化的模型以及外扰的估计不同,所提出动力学自抗扰方法可以实现UUV动态变化模型、外部干扰以及速度信息的同时估计,有利于实现UUV的稳定控制.

1 问题描述

本文研究的UUV,推进器布置在艉部用于实现对前向速度的控制,垂直舵用于实现对艏向角的控制,水平舵用于实现对俯仰角的控制,由此可知,UUV空间运动的状态变量多于控制输入,因此本文的研究对象是一个多变量、非线性、强耦合的欠驱动系统[31]. 本文建立流体坐标系$\{A_i\}$、固定坐标系$\{I\}$、Serret-Frenet坐标系$\{F_i\}$对UUV和预设路径进行描述,如图1所示.

由于正常航行时横摇对UUV的运动影响很小,通常可忽略横摇作用,只考虑5个自由度,本文采用文献[32]提出的UUV模型和相关参数,即质量、水动力系数、稳心高等. 第i艘UUV在三维空间的运动可以用五自由度模型表示为如下运动学方程:

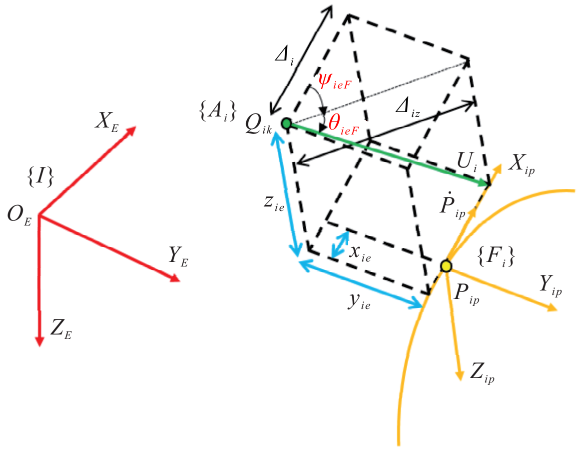

图 1　参考坐标系

$$\begin{cases} \dot{x}_i = U_i \cos \varPsi_i \cos \varTheta_i,\ \dot{y}_i = U_i \sin \varPsi_i \cos \varTheta_i, \\ \dot{z}_i = -U_i \sin \varTheta_i,\ \dot{\varTheta}_i = q_i - \dot{\alpha}_i, \\ \dot{\varPsi}_i = r_i / \cos \theta_i + \dot{\beta} \end{cases} \quad (1)$$

和动力学方程

$$\begin{cases} m_{iu}\dot{u}_i = f_{iu}(\cdot) + \tau_{iu} + d_{iu}, \\ m_{iv}\dot{v}_i = f_{iv}(\cdot) + d_{iv}, m_{iw}\dot{w}_i = f_{iw}(\cdot) + d_{iw}, \\ m_{iq}\dot{q}_i = f_{iq}(\cdot) + \tau_{iq} + d_{iq}, \\ m_{ir}\dot{r}_i = f_{ir}(\cdot) + \tau_{ir} + d_{ir}. \end{cases} \quad (2)$$

其中: x_i、y_i、z_i 为固定坐标系 $\{I\}$ 下 UUV 的位置; $U_i = \sqrt{u_i^2 + v_i^2 + w_i^2}$ 为 UUV 的总速度; $\varTheta_i = \theta_i - \alpha_i$, $\varPsi_i = \psi_i + \beta_i$ 分别为 UUV 的航迹角和方位角; θ_i、ψ_i 分别为 UUV 的俯仰角和航向角; $\alpha_i = \arctan(w_i/u_i)$、$\beta_i = \arcsin(v_i/U_i)$ 分别为 UUV 的攻角和侧滑角, $u_i > 0$, u_i、v_i、w_i、q_i 和 r_i 分别为船体坐标系下 UUV 的前向速度、横向速度、垂向速度、纵倾角速度和艏摇角速度; τ_{iu}、τ_{iq} 和 τ_{ir} 分别为欠驱动 UUV 的推力、纵倾力矩和艏摇力矩; d_{iu}、d_{iv}、d_{iw}、d_{iq} 和 d_{ir} 为未知外部环境扰动. 另有

$$\begin{aligned} & f_{iu}(\cdot) = m_{iv}v_i r_i - m_{iw}w_i q_i - X_{iu}u_i - X_{iu|u|}u_i|u_i|, \\ & f_{iv}(\cdot) = m_{iu}u_i r_i - Y_{iv}v_i - Y_{iv|v|}v_i|v_i|, \\ & f_{iw}(\cdot) = m_{iu}u_i q_i - Z_{iw}w_i - Z_{iw|w|}w_i|w_i|, \\ & f_{iq}(\cdot) = (m_{iw} - m_{iu})u_i w_i - M_{iq}q_i - M_{iq|q|}q_i|q_i| - \\ & \qquad (\overline{B_i G_{iz}} W_i) \sin \theta_i, \\ & f_{ir}(\cdot) = (m_{iu} - m_{iv})u_i v_i - N_{ir}r_i - N_{ir|r|}r_i|r_i|. \end{aligned}$$

其中: $m_{(\cdot)}$ 为 UUV 质量和由流体惯性作用产生的附加质量; $X_{(\cdot)}, Y_{(\cdot)}, Z_{(\cdot)}, M_{(\cdot)}, N_{(\cdot)}$ 为流体黏性力水动力系数; $\overline{B_i G_{iz}} W_i = z_{iG}W_i - z_{iB}B_i$, z_{iG} 和 z_{iB} 分别为 UUV 的重心和浮心位置, W_i 和 B_i 分别为 UUV 的重力和浮力, $\overline{B_i G_{iz}}$ 为重心与浮心之间的距离.

定义第 i 艘欠驱动 UUV 的参数化路径为 $P_{id}(\chi_i) = (x_{id}(\chi_i), y_{id}(\chi_i), z_{id}(\chi_i))$, 其中 χ_i 为路径参数, 则预设路径的切线角可描述为

$$\theta_{id}(\chi_i) = \arctan(-z'_{id}(\chi_i)/\sqrt{x'^2_{id}(\chi_i) + y'^2_{id}(\chi_i)}),$$
$$\psi_{id}(\chi_i) = \arctan(y'_{id}(\chi_i)/x'_{id}(\chi_i)).$$

其中

$$\begin{aligned} x'_{id}(\chi_i) &= \partial x_{id}/\partial \chi_i, \\ y'_{id}(\chi_i) &= \partial y_{id}/\partial \chi_i, \\ z'_{id}(\chi_i) &= \partial z_{id}/\partial \chi_i. \end{aligned}$$

定义 $R^I_{F_i}$ 为从 $\{F_i\}$ 到 $\{I\}$ 的旋转矩阵, 则有

$$R^I_{F_i} = \begin{bmatrix} \cos \theta_{id} \cos \varphi_{id} & -\sin \theta_{id} & \sin \theta_{id} \cos \varphi_{id} \\ \cos \theta_{id} \cos \varphi_{id} & \cos \varphi_{id} & \sin \theta_{id} \sin \varphi_{id} \\ -\sin \theta_{id} & 0 & \cos \theta_{id} \end{bmatrix}.$$

定义路径跟踪误差 $\varepsilon_i = [x_{ie}, y_{ie}, z_{ie}]^{\mathrm{T}}$, 则有

$$\varepsilon_i = R^{I\ \mathrm{T}}_{F_i}(\eta_i - \eta_{id}). \quad (3)$$

其中

$$\eta_{id} = [x_{id}(\chi_i), y_{id}(\chi_i), z_{id}(\chi_i)]^{\mathrm{T}},\ \eta_i = [x_i, y_i, z_i]^{\mathrm{T}}.$$

对 ε_i 求导可得

$$\dot{\varepsilon}_i = \dot{R}^{I\mathrm{T}}_{F_i}(\eta_i - \eta_{id}) + R^{I\mathrm{T}}_{F_i}(\dot{\eta}_i - \dot{\eta}_{id}). \quad (4)$$

其中: $\dot{R}^I_{F_i} = R^I_{F_i} S_{F_i}$, 且有

$$S_{F_i} = \begin{bmatrix} 0 & -\dot{\psi}_{id} \cos \theta_{id} & \dot{\theta}_{id} \\ \dot{\psi}_{id} \cos \theta_{id} & 0 & \dot{\psi}_{id} \sin \theta_{id} \\ -\dot{\theta}_{id} & -\dot{\psi}_{id} \sin \theta_{id} & 0 \end{bmatrix}. \quad (5)$$

定义 $R^F_{A_i}$ 为 $\{A_i\}$ 到 $\{F_i\}$ 的旋转矩阵, 则有

$$\dot{\eta}_i = R^I_{F_i} R^F_{Ai} U_{iA}. \quad (6)$$

其中: $\psi_{ieF} = \arctan(-y_{ie}/\Delta_i)$, $\theta_{ieF} = \arctan(z_{ie}/\Delta_{iz})$, $R^F_{A_i} = [\cos \theta_{ieF} \cos \psi_{ieF}, -\sin \psi_{ieF}, \sin \theta_{ieF} \cos \psi_{ieF}; \cos \theta_{ieF} \sin \psi_{ieF}, \cos \psi_{ieF}, \sin \theta_{ieF} \sin \psi_{ieF}; -\sin \theta_{ieF}, 0, \cos \theta_{ieF}]$; $U_{iA} = [U_i, 0, 0]^{\mathrm{T}}$ 为第 i 个 UUV 在 $\{A_i\}$ 中的速度; Δ_i 为水平前视距离; $\Delta_{iz} = \lambda_i \sqrt{\Delta_i^2 + y_{ie}^2}$ 为竖直前视距离, λ_i 为正常数.

需要注意的是, 在传统 LOS 制导中 Δ_i 通常为固定值, 其数值大小需要反复调试整定, 当跟踪的路径比较复杂时容易引起超调和震荡. 为解决上述问题, 本文设计自适应前视距离策略, 具体如下:

$$\Delta_i = \frac{2(\Delta_{i\max} - \Delta_{i\min})}{1 + \mathrm{e}^{(k_{ia} y_{ie}^2)}} + \Delta_{i\min}. \quad (7)$$

其中: $\Delta_{i\max}$、$\Delta_{i\min}$ 分别为最大前视距离和最小前视距离, 可根据跟踪路径的复杂程度整体设定; k_{ia} 为调节系数, 其值越大前视距离的变化幅度越大, 反之越小. 由式 (7) 可以看出: 当跟踪的横向误差较大时, Δ_i

将取较小值以提高UUV的跟踪偏差收敛速度; 当横向偏差变小时, Δ_i 将取较大值以确保跟踪平滑, 有效防止超调和震荡.

将式(6)代入(4), 可得

$$\dot{\varepsilon}_i = S_{F_i}^{\mathrm{T}}\varepsilon_i + R_{A_i}^{F}U_{iA} - F_{F_i}^{\mathrm{IT}}\dot{\eta}_{id}. \tag{8}$$

则UUV的三维路径跟踪误差动态为

$$\begin{cases}\dot{x}_{ie} = U_i\cos\varphi_{ieF}\cos\theta_{ieF} + \dot{\psi}_{id}\cos\theta_{id}y_{ie} - \\ \qquad \dot{\theta}_{id}z_{ie} - U_{id}^{*}\dot{\chi}_i, \\ \dot{y}_{ie} = U_i\sin\varphi_{ieF}\cos\theta_{ieF} - \dot{\psi}_{id}\cos\theta_{id}x_{ie} - \\ \qquad \dot{\psi}_{id}\sin\theta_{id}z_{ie}, \\ \dot{z}_{ie} = -U_i\sin\theta_{ieF} + \dot{\theta}_{id}x_{ie} + \dot{\psi}_{id}\sin\theta_{id}y_{ie},\end{cases} \tag{9}$$

其中 $U_{id}^{*} = \sqrt{x'^2_{id}(\chi_i) + y'^2_{id}(\chi_i) + z'^2_{id}(\chi_i)}$.

2 控制器设计

欠驱动UUV的三维协同路径跟踪控制包括运动学制导和动力学控制两部分.

2.1 运动学控制律设计

在运动控制环节, 提出三维ALOS制导律, 设计制导前向速度 U_{iU}、制导航迹角 $\Theta_{i\theta}$、制导方位角 $\Psi_{i\psi}$、俯仰角速度 q_{iq}、艏摇角速度 r_{ir} 等制导指令. 定义

$$\begin{cases}U_{ie} = U_i - U_{iU},\ \theta_{ie} = \theta_i - \alpha_i - \Theta_{i\theta}, \\ \Psi_{ie} = \psi_i + \beta_i - \Psi_{i\psi},\ q_{ie} = q_i - q_{iq}, \\ r_{ie} = r_i - r_{ir},\ \dot{\chi}_i = v_s - \omega_i.\end{cases} \tag{10}$$

其中: v_s 为恒正的参考速度, ω_i 为后续要设计的变量.

令 $\hat{U}_{ie}$、$\hat{q}_{ie}$ 和 $\hat{r}_{ie}$ 分别为 U_{ie}、q_{ie} 和 r_{ie} 的估计, 则估计误差可定义为

$$\begin{cases}\tilde{U}_{ie} = \hat{U}_{ie} - U_{ie}, \\ \tilde{q}_{ie} = \hat{q}_{ie} - q_{ie}, \\ \tilde{r}_{ie} = \hat{r}_{ie} - r_{ie}.\end{cases} \tag{11}$$

由式(10)和(11)可知, 式(9)可写为

$$\begin{cases}\dot{x}_{ie} = U_{iU} + \tilde{U}_{ie} - U_i(1-\cos\psi_{ieF}\cos\theta_{ieF}) - \\ \qquad \tilde{U}_i + \dot{\psi}_{id}\cos\theta_{id}y_{ie} - \dot{\theta}_{id}z_{ie} - U_{id}^{*}\dot{\chi}_i, \\ \dot{y}_{ie} = U_i\sin\psi_{ieF}\cos\theta_{ieF} - \dot{\psi}_{id}\cos\theta_{id}x_{ie} - \\ \qquad \dot{\psi}_{id}\sin\theta_{id}z_{ie}, \\ \dot{z}_{ie} = -U_i\sin\theta_{ieF} + \dot{\theta}_{id}x_{ie} + \dot{\psi}_{id}\sin\theta_{id}y_{ie}, \\ \dot{\Theta}_{ie} = q_{iq} + \tilde{q}_{ie} - \tilde{q}_i - \dot{\alpha}_i - \dot{\Theta}_{i\theta}, \\ \dot{\Psi}_{ie} = (r_{ir} + \tilde{r}_{ie} - \tilde{r}_i)/\cos\theta_i + \beta_i - \dot{\Psi}_{i\psi}.\end{cases} \tag{12}$$

设计ALOS制导律为

$$\begin{cases}U_{iU} = -k_{i1}x_{ie}/\Pi_{ix} - \hat{U}_{ie} + U_{id}^{*}v_s + \\ \qquad U_i(1-\cos\psi_{ieF}\cos\theta_{ieF}), \\ q_{iq} = -k_{i2}\Theta_{ie}/\Pi_{i\theta} - \hat{q}_{ie} + \dot{\alpha} + \dot{\Theta}_{i\theta}, \\ r_{ir} = -k_{i3}\Psi_{ie}\cos\theta_i/\Pi_{i\psi} - \hat{r}_{ie} - \\ \qquad (\dot{\beta} - \dot{\Psi}_{i\psi})\cos\theta_i, \\ \Psi_{i\psi} = \psi_{id} + \psi_{ieF},\ \Theta_{i\theta} = \theta_{id} + \theta_{ieF}.\end{cases} \tag{13}$$

其中: $\Pi_{i\psi} = \sqrt{\Psi_{ie}^2 + \Delta_{i\psi}^2}$, $\Pi_{i\theta} = \sqrt{\Theta_{ie}^2 + \Delta_{i\theta}^2}$, $\Pi_{ix} = \sqrt{x_{ie}^2 + \Delta_{ix}^2}$, k_{i1}、k_{i2}、k_{i3}、Δ_{ix}、$\Delta_{i\theta}$ 和 $\Delta_{i\psi}$ 为正常数.

将式(13)代入(12), 有

$$\begin{cases}\dot{x}_{ie} = -k_{i1}x_{ie}/\Pi_{ix} + U_{id}^{*}\omega_i + \\ \qquad \dot{\psi}_{id}\cos\theta_{id}y_{ie} - \dot{\theta}_{id}z_{ie} - \tilde{U}_{ie}, \\ \dot{y}_{ie} = -U_i\cos\theta_{ieF}y_{ie}/\Pi_{iy} - \\ \qquad \dot{\psi}_{id}\cos\theta_{id}x_{ie} - \dot{\psi}_{id}\sin\theta_{id}z_{ie}, \\ \dot{z}_{ie} = -U_iz_{ie}/\Pi_{iz} + \dot{\theta}_{id}x_{ie} + \dot{\psi}_{id}\sin\theta_{id}y_{ie}, \\ \dot{\Theta}_{ie} = -k_{i2}\Theta_{ie}/\Pi_{i\theta} - \tilde{q}_{ie}, \\ \dot{\Psi}_{ie} = -k_{i3}\Psi_{ie}/\Pi_{i\psi} - \tilde{r}_{ie}/\cos\theta_i.\end{cases} \tag{14}$$

其中: $\Pi_{iy} = \sqrt{y_{ie}^2 + \Delta_i^2}$, $\Pi_{iz} = \sqrt{z_{ie}^2 + \Delta_{iz}^2}$.

为实现欠驱动UUV集群的协同控制, 定义协同误差为

$$e_i = \sum_{j=1}^{N} a_{ij}(\chi_i - \chi_j). \tag{15}$$

定义 $e = [e_1, \dots, e_N]^{\mathrm{T}}$, $\chi = [\chi_1, \dots, \chi_N]^{\mathrm{T}}$, 则有 $e = \mathcal{L}\chi$. ω_i 可写为

$$\omega_i = \mu_ie_i - \mu_iU_{id}^{*}x_{ie}, \tag{16}$$

其中 μ_i 为正常数.

定义 $\omega = [\omega_1, \dots, \omega_N]^{\mathrm{T}}$, 得到跟踪误差子系统

$$\begin{cases}\dot{x}_{ie} = -k_{i1}x_{ie}/\Pi_{ix} + U_{id}^{*}\omega_i + \\ \qquad \dot{\psi}_{id}\cos\theta_{id}y_{ie} - \dot{\theta}_{id}z_{ie} - \tilde{U}_{ie}, \\ \dot{y}_{ie} = -U_i\cos\theta_{ieF}y_{ie}/\Pi_{iy} - \\ \qquad \dot{\psi}_{id}\cos\theta_{id}x_{ie} - \dot{\psi}_{id}\sin\theta_{id}z_{ie}, \\ \dot{z}_{ie} = -U_iz_{ie}/\Pi_{iz} + \dot{\theta}_{id}x_{ie} + \dot{\psi}_{id}\sin\theta_{id}y_{ie}, \\ \dot{\Theta}_{ie} = -k_{i2}\Theta_{ie}/\Pi_{i\theta} - \tilde{q}_{ie}, \\ \dot{\Psi}_{ie} = -k_{i3}\Psi_{ie}/\Pi_{i\psi} - \tilde{r}_{ie}/\cos\theta_i, \\ \dot{e} = -\mathcal{L}\omega.\end{cases} \tag{17}$$

2.2 动力学控制律设计

由$u_i=U_i\cos\alpha_i\cos\beta_i$,可将式(2)改写为

$$\begin{cases}\dot{U}_i=f_{iU}+b_{iU}\tau_{iu},\\ \dot{q}_i=f_{iq}+b_{iq}\tau_{iq},\\ \dot{r}_i=f_{ir}+b_{ir}\tau_{ir}.\end{cases}\tag{18}$$

其中:b_{iU}、b_{iq}和b_{ir}为控制增益;$|\tau_{iu}|\leqslant\tau_{iu}^*$,$|\tau_{iq}|\leqslant\tau_{iq}^*$,$|\tau_{ir}|\leqslant\tau_{ir}^*$;$f_{iU}=m_{iu}^{-1}(f_{iu}(\cdot)+\dot{U}_i(\sin^2(\alpha_i+\beta_i)/2+\sin^2(\alpha_i-\beta_i)/2)+U_i\sin\alpha_i\cos\beta_i\dot{\alpha}_i+U_i\cos\alpha_i\sin\beta_i\dot{\beta}_i+d_{iu})$,且有$|f_{iU}|\leqslant f_{iU}^*$;$f_{iq}=m_{iq}^{-1}[f_{iq}(\cdot)+d_{iq}]$,且有$|f_{iq}|\leqslant f_{iq}^*$; $f_{ir}=m_{ir}^{-1}[f_{ir}(\cdot)+d_{ir}]$,且有$|f_{ir}|\leqslant f_{ir}^*$;$\tau_{iU}^*$、$\tau_{iq}^*$、$\tau_{ir}^*$、$f_{iU}^*$、$f_{iq}^*$和$f_{ir}^*$均为正常数.

令

$$\tilde{U}_i=\hat{U}_i-U_i,\ \tilde{q}_i=\hat{q}_i-q_i,\ \tilde{r}_i=\hat{r}_i-r_i,$$

设计线性ESO为

$$\begin{cases}\dot{\hat{U}}_i=\hat{f}_{iU}+b_{iU}\tau_{iu}-\beta_{iU1}\tilde{U}_i,\dot{\hat{f}}_{iU}=-\beta_{iU2}\tilde{U}_i;\\ \dot{\hat{q}}_i=\hat{f}_{iq}+b_{iq}\tau_{iq}-\beta_{iq1}\tilde{q}_i,\dot{\hat{f}}_{iq}=-\beta_{iq2}\tilde{q}_i;\\ \dot{\hat{r}}_i=\hat{f}_{ir}+b_{ir}\tau_{ir}-\beta_{ir1}\tilde{r}_i,\dot{\hat{f}}_{ir}=-\beta_{ir2}\tilde{r}_i.\end{cases}\tag{19}$$

其中:$\hat{U}_i$、$\hat{q}_i$、$\hat{r}_i$、$\hat{f}_{iU}$、$\hat{f}_{iq}$、$\hat{f}_{ir}$分别为U_i、q_i、r_i、f_{iU}、f_{iq}、f_{ir}的估计值,β_{iU1}、β_{iU2}、β_{iq1}、β_{iq2}、β_{ir1}、β_{ir2}为ESO的观测器增益.

令

$$\tilde{f}_{iU}=\hat{f}_{iU}-f_{iU},\ \tilde{f}_{iq}=\hat{f}_{iq}-f_{iq},\ \tilde{f}_{ir}=\hat{f}_{ir}-f_{ir},$$

则有

$$\begin{cases}\dot{\tilde{U}}_i=-\beta_{iU1}\tilde{U}_i+\tilde{f}_{iU},\dot{\tilde{f}}_{iU}=-\beta_{iU2}\tilde{U}_i-\dot{f}_{iU};\\ \dot{\tilde{q}}_i=-\beta_{iq1}\tilde{q}_i+\tilde{f}_{iq},\dot{\tilde{f}}_{iq}=-\beta_{iq2}\tilde{q}_i-\dot{f}_{iq};\\ \dot{\tilde{r}}_i=-\beta_{ir1}\tilde{r}_i+\tilde{f}_{ir},\dot{\tilde{f}}_{ir}=-\beta_{ir2}\tilde{r}_i-\dot{f}_{ir}.\end{cases}\tag{20}$$

令$E_{i2}=[\tilde{U}_i,\tilde{f}_{iU},\tilde{q}_i,\tilde{f}_{iq},\tilde{r}_i,\tilde{f}_{ir}]^{\mathrm{T}}$,可得估计误差子系统

$$\dot{E}_{i2}=A_{i1}E_{i2}-B_{i1}\dot{f}_i.\tag{21}$$

其中

$$A_{i1}=[-\beta_{iu1},1,0,0,0,0;-\beta_{iu2},0,0,0,0,0;\\ 0,0,-\beta_{ir2},1,0,0;0,0,-\beta_{iq2},0,0,0;\\ 0,0,0,0,\beta_{ir1},1;0,0,0,0,-\beta_{ir2},0].$$

$$B_{i1}=[0,0,0;1,0,0;0,0,0;0,1,0;0,0,0;0,0,1].$$

$$\dot{f}_i=[\dot{f}_{iU},\dot{f}_{iq},\dot{f}_{ir}]^{\mathrm{T}}.$$

由于A_{i1}为Hurwitz阵,存在正定矩阵P_{i1}满足

$$A_{i1}^{\mathrm{T}}P_{i1}+P_{i1}A_{i1}=-\varepsilon_{iU}I_1,\tag{22}$$

其中ε_{iU}为正常数.

令

$$\hat{U}_{ie}=\hat{U}_i-U_{iU},\ \hat{q}_{ie}=\hat{q}_i-q_{iq},\ \hat{r}_{ie}=\hat{r}_i-r_{ir},$$

对其求导可得

$$\begin{cases}\dot{\hat{U}}_{ie}=-\beta_{iU1}\tilde{U}_i+\hat{f}_{iU}+b_{iU}\tau_{iu}-\dot{U}_{iU},\\ \dot{\hat{q}}_{ie}=-\beta_{iq1}\tilde{q}_i+\hat{f}_{iq}+b_{iq}\tau_{iq}-\dot{q}_{iq},\\ \dot{\hat{r}}_{ie}=-\beta_{ir1}\tilde{r}_i+\hat{f}_{ir}+b_{ir}\tau_{ir}-\dot{r}_{ir}.\end{cases}\tag{23}$$

第i艘UUV的控制律可设计为

$$\begin{cases}\tau_{iU}=b_{iU}^{-1}[k_{iUp}(U_{iU}-\hat{U}_i)-\hat{f}_{iU}],\\ \tau_{iq}=b_{iq}^{-1}[k_{iqp}(q_{iq}-\hat{q}_i)-\hat{f}_{iq}],\\ \tau_{ir}=b_{ir}^{-1}[k_{irp}(r_{ir}-\hat{r}_i)-\hat{f}_{ir}].\end{cases}\tag{24}$$

其中k_{iUp}、k_{iqp}、k_{irp}为控制增益.

将式(24)代入(23),得到控制误差子系统

$$\begin{cases}\dot{\hat{U}}_{ie}=-k_{iUp}\hat{U}_{ie}-\beta_{iU1}\tilde{U}_i-\dot{U}_{iU},\\ \dot{\hat{q}}_{ie}=-k_{iqp}\hat{q}_{ie}-\beta_{iq1}\tilde{q}_i-\dot{q}_{iq},\\ \dot{\hat{r}}_{ie}=-k_{irp}\hat{r}_{ie}-\beta_{ir1}\tilde{r}_i-\dot{r}_{ir}.\end{cases}\tag{25}$$

3 稳定性分析

三维协同路径跟踪控制系统是由跟踪误差子系统(17)、估计误差子系统(21)和控制误差子系统(25)构成的级联系统.

引理1用来证明子系统(17)的稳定性.

引理1 子系统(17)可看作一个状态为x_{ie}、y_{ie}、z_{ie}、$\varTheta_{ie}$、$\varPsi_{ie}$、e,输入为$\tilde{U}_{ie}$、$\tilde{q}_{ie}$、$\tilde{r}_{ie}$的系统,则该系统是输入状态稳定的.

证明 构建Lyapunov函数

$$V_1=\frac{1}{2}\sum_{i=1}^N\{x_{ie}^2+y_{ie}^2+z_{ie}^2+\varTheta_{ie}^2+\varPsi_{ie}^2\}+\chi^{\mathrm{T}}\mathcal{L}\chi.$$

由文献[33]可知

$$V_1=\sum_{i=1}^N\{x_{ie}^2+y_{ie}^2+z_{ie}^2+\varTheta_{ie}^2+\varPsi_{ie}^2\}+e^{\mathrm{T}}Pe.$$

对其求导,并将式(17)代入可得

$$\dot{V}_1=\\ \sum_{i=1}^N\Big\{-\frac{k_{i1}x_{ie}^2}{\varPi_{ix}}-\frac{U_i\cos\theta_{ieF}y_{ie}^2}{\varPi_{iy}}-\frac{U_iz_{ie}^2}{\varPi_{iz}}-\frac{k_{i2}\varTheta_{ie}^2}{\varPi_{i\theta}}-\\ \frac{k_{i3}\varPsi_{ie}^2}{\varPi_{i\psi}}-\tilde{U}_{ie}x_{ie}-\tilde{q}_{ie}\varTheta_{ie}-\frac{\tilde{r}_{ie}\varPsi_{ie}}{\cos\theta_i}-\frac{\mu_i\varPi_{ie}\vartheta_{ie}^2}{\varPi_{ie}}\Big\}.$$

其中:$\vartheta_{ie}=U_{id}^*x_{ie}-e_i$,$\varPi_{ie}=\sqrt{\vartheta_{ie}^2+\varDelta_{i\vartheta}^2}$,$\varDelta_{i\vartheta}$为常数.

定义$E'_{i1}=[x_{ie},y_{ie},z_{ie},\Theta_{ie},\Psi_{ie},\vartheta_{ie}]^{\mathrm{T}}$,则有

$$\dot V_1\leqslant\sum_{i=1}^{N}\Big\{-\frac{\lambda_{\min}(K_{i1})\|E'_{i1}\|^2}{\sqrt{\|E'_{i1}\|^2+\Delta_{i\max}^2}}+\|h_{i1}\|\|E'_{i1}\|\Big\}.$$

其中: $\lambda_{\min}(\cdot)$为矩阵的最小特征值, $K_{i1}=\mathrm{diag}\{k_{i1},U_i\cos\theta_{ieF},U_i,k_{i2},k_{i3},\mu_i\Pi_{ie}\}$, $h_{i1}=[-\tilde U_{ie},0,0,-\tilde q_{ie},-\tilde r_{ie}/\cos\theta,0]^{\mathrm{T}}$, $\Delta_{i\max}=\max\{\Delta_{ix},\Delta_{iy},\Delta_{iz},\Delta_{i\theta},\Delta_{i\psi},\Delta_{i\vartheta}\}$.

因为$\dfrac{\|E'_{i1}\|}{\sqrt{\|E'_{i1}\|^2+\Delta_{i\max}^2}}\geqslant\dfrac{\|h_{i1}\|}{\bar\rho_{i1}\lambda_{\min}(K_{i1})}$,可得

$$\dot V_1\leqslant\sum_{i=1}^{N}\Big\{-\frac{(1-\bar\rho_{i1})\lambda_{\min}(K_{i1})\|E'_{i1}\|^2}{\sqrt{\|E'_{i1}\|^2+\Delta_{i\max}^2}}\Big\},$$

其中$0<\bar\rho_{i1}<1$.

定义$E_{i1}=[x_{ie},y_{ie},z_{ie},\Theta_{ie},\Psi_{ie},e_i]^{\mathrm{T}}$,则有$E'_{i1}=\varphi_iE_{i1}$,其中

$$\varphi_i=[1,0,0,0,0,0;0,1,0,0,0,0;0,0,1,0,0,0;0,0,0,1,0,0;0,0,0,0,1,0;U_{id}^*,0,0,0,0,-1].$$

由于$U_{id}^*>0$,可以计算出$0<\lambda_{\min}(\varphi_i)<1$.

由于$\|E'_{i1}\|\geqslant\lambda_{\min}(\varphi_i)E_{i1}$,可得

$$\dot V_1\leqslant\sum_{i=1}^{N}\Big\{-\frac{(1-\bar\rho_{i1})\lambda_{\min}(K_{i1})\lambda_{\min}(\varphi_i)\|E_{i1}\|^2}{\sqrt{\|E_{i1}\|^2+\Delta_{i\max}^2}}\Big\}.$$

由此可知,跟踪误差子系统(17)是级联稳定的,且存在$\mathcal{KL}$类函数$\alpha_{i1}(\cdot)$和$\mathcal{K}_\infty$类函数$\iota_i^{h_1}(\cdot)$满足

$$\|E_{i1}(t)\|\leqslant\alpha_{i1}(E_{i1}(t_0),t-t_0)+\iota_i^{h_1}\|h_{i1}\|.$$

其中: $S_{i1}=\mathrm{diag}\{1,P\}$, $\iota_i^{h_1}(s)=\varpi_i^{-1}(\sqrt{\lambda_{\max}(S_{i1})}s/(\bar\rho_{i1}\lambda_{\min}(K_{i1})\lambda_{\min}(\varphi_i)\sqrt{\lambda_{\min}(S_{i1})}))$.

由文献[33]可知

$$e^{\mathrm{T}}Pe\geqslant\lambda^*\Big\|-1_N\frac{1}{N}\sum_{i=1}^{N}\chi_i\Big\|^2.$$

由于e_i有界,使得$\chi_i\to\chi_j\to\dfrac{1}{N}\sum\limits_{i=1}^{N}\chi_i$,从而实现了UUV的协同控制. □

引理2用来证明子系统(21)的稳定性.

引理2　子系统(21)可看作一个状态为$\tilde U_i$、$\tilde f_{iU}$、$\tilde q_i$、$\tilde f_{iq}$、$\tilde r_i$、$\tilde f_{ir}$,输入为$\dot f_{iU}$、$\dot f_{iq}$、$\dot f_{ir}$的系统,则该系统是输入状态稳定的.

证明　构建Lyapunov函数$V_2=\dfrac{1}{2}E_{i2}^{\mathrm{T}}P_{i1}E_{i2}$,对$V_2$求导可得$\dot V_2\leqslant\|E_{i2}\|\|P_{i1}B_{i1}\|\|\dot f_i\|-\dfrac{\varepsilon_{iu}}{2}\|E_{i2}\|^2$,其中$\varepsilon_{iu}=\min\{\varepsilon_1,\varepsilon_2,\varepsilon_3,\varepsilon_4,\varepsilon_5,\varepsilon_6\}$. 由$\|E_{i2}\|\geqslant\dfrac{2\|P_{i1}B_{i1}\|\|\dot f_i\|}{\varepsilon_{iu}\bar\rho_{i2}}$可得

$$\dot V_2\leqslant-\frac{\varepsilon_{iu}}{2}(1-\bar\rho_{i2})\|E_{i2}\|^2,$$

其中$0<\bar\rho_{i2}<1$. 因此估计误差子系统(21)是输入状态稳定的,且存在$\mathcal{KL}$类函数$\alpha_{i2}(\cdot)$和$\mathcal{K}_\infty$类函数$\iota_i^{h_2}(\cdot)$满足

$$\|E_{i2}(t)\|\leqslant\alpha_{i2}(E_{i2}(t_0),t-t_0)+\iota_i^{h_2}(\|f_i\|),$$

其中

$$\iota_i^{h_2}(s)=2\sqrt{\lambda_{\min}(P_{i1})}\|P_{i1}B_{i1}\|s/\sqrt{\lambda_{\min}(P_{i1})\varepsilon_{iu}\bar\rho_{i2}}.$$ □

引理3用来证明子系统(25)的稳定性.

引理3　子系统(25)可看作一个状态为$\hat U_{ie}$、$\hat q_{ie}$、$\hat r_{ie}$,输入为$\tilde U_i$、$\tilde q_i$、$\tilde r_i$的系统,则该系统是输入状态稳定的.

证明　构建Lyapunov函数

$$V_3=\frac{1}{2}\hat U_{ie}^2+\frac{1}{2}\hat q_{ie}^2+\frac{1}{2}\hat r_{ie}^2,$$

对V_3求导得$\dot V_3=\hat U_{ie}\dot{\hat U}_{ie}+\hat q_{ie}\dot{\hat q}_{ie}+\hat r_{ie}\dot{\hat r}_{ie}$,将式(25)代入可得

$$\dot V_3\leqslant-k_{iUp}\hat U_{ie}^2+\beta_{iU1}|\hat U_{ie}||\tilde U_i|-k_{iqp}\hat q_{ie}^2+\beta_{iq1}|\hat q_{ie}||\tilde q_i|-k_{irp}\hat r_{ie}^2+\beta_{ir1}|\hat r_{ie}||\tilde r_i|.$$

其中

$$\hat U_{ie}>\frac{\beta_{iU1}|\tilde U_i|}{k_{iUp}\bar\rho_{i3}},\ \hat q_{ie}>\frac{\beta_{iq1}|\tilde q_i|}{k_{iqp}\bar\rho_{i4}},\ \hat r_{ie}>\frac{\beta_{ir1}|\tilde r_i|}{k_{irp}\bar\rho_{i5}},$$

$$0<\bar\rho_{i3}<1,\ 0<\bar\rho_{i4}<1,\ 0<\bar\rho_{i5}<1.$$

则有

$$\dot V_3\leqslant-k_{iUp}(1-\bar\rho_{i3})|\hat U_{ie}|-k_{iqp}(1-\bar\rho_{i4})|\hat q_{ie}|-k_{irp}(1-\bar\rho_{i5})|\hat r_{ie}|.$$

由此可知控制误差子系统是输入状态稳定的,且存在如下$\mathcal{KL}$类函数$\alpha(\cdot)$和$\mathcal{K}_\infty$类函数$\gamma(\cdot)$,使得

$$|\hat U_{ie}|\leqslant\alpha_1(\hat U_{ie}(t_0),t-t_0)+\gamma_1(|\tilde U_i|),$$
$$\gamma_1(s)=\beta_{iU1}s/(k_{iUp}\bar\rho_{i3}),$$
$$|\hat q_{ie}|\leqslant\alpha_2(\hat q_{ie}(t_0),t-t_0)+\gamma_2(|\tilde q_i|),$$
$$\gamma_2(s)=\beta_{iq1}s/(k_{iqp}\bar\rho_{i4}),$$
$$|\hat r_{ie}|\leqslant\alpha_3(\hat r_{ie}(t_0),t-t_0)+\gamma_3(|\tilde r_i|),$$
$$\gamma_3(s)=\beta_{ir1}s/(k_{irp}\bar\rho_{i5}).$$ □

定理1用来证明闭环系统的稳定性.

定理1　跟踪误差子系统(17)、估计误差子系统(21)和控制误差子系统(25)组成的闭环系统是输入状态稳定的.

证明　由引理1～引理3可知,以$\tilde U_{ie}$、$\tilde q_{ie}$、$\tilde r_{ie}$为输入的子系统(17)是输入状态稳定的,以$\dot f_{iU}$、$\dot f_{iq}$、$\dot f_{ir}$为输入的子系统(21)是输入状态稳定的,以$\tilde U_i$、$\tilde q_i$、$\tilde r_i$为输入的子系统(25)是输入状态稳定的. 根据文献

[34]可知,这3个子系统可看作一个状态为x_{ie}、y_{ie}、z_{ie}、Θ_{ie}、Ψ_{ie}、e、$\hat{U}_{ie}$、$\hat{q}_{ie}$、$\hat{r}_{ie}$、$\tilde{f}_{iU}$、$\tilde{f}_{iq}$、$\tilde{f}_{ir}$,输入为$\tilde{U}_{ie}, \tilde{q}_{ie}, \tilde{r}_{ie}, \dot{f}_{iU}, \dot{f}_{iq}, \dot{f}_{ir}$的级联系统,且整个系统是输入状态稳定的. □

4 仿真结果分析

为验证所提出基于自适应视距制导的无人潜航器三维协同路径跟踪控制方法的有效性,本节针对由三艘UUV组成的无人集群进行仿真分析. 环境扰动建模为一阶高斯-马尔可夫过程,表示为

$$\dot{d}_{ik} + \gamma_{ik} d_{ik} = w_k,\ \gamma_{ik} > 0.$$

其中: $k = [u, v, w, q, r]$, w_k为白噪声. 协同路径跟踪控制器的参数选择如下:

$$k_{i1} = 0.1,\ k_{i2} = 1,\ k_{i3} = 1,$$
$$\nu_s = 0.1,\ \beta_{iU1} = 15,\ \beta_{iU2} = 200,$$
$$\beta_{iq1} = 15,\ \beta_{iq2} = 200,\ \beta_{ir1} = 15,$$
$$\beta_{ir2} = 200,\ k_{iUp} = 200,\ k_{iqp} = 80,$$
$$k_{irp} = 80,\ \Delta_{i\min} = 1,\ \Delta_{i\max} = 10,$$
$$k_{ia} = 5,\ \lambda_i = 0.5.$$

3艘UUV的初始位置状态信息分别为

$$(x_1, y_1, z_1, \Theta_1, \Psi_1) = (0, 20, 0, 0, 0),$$
$$(x_2, y_2, z_2, \Theta_2, \Psi_2) = (0, -30, 0, 0, 0),$$
$$(x_3, y_3, z_3, \Theta_3, \Psi_3) = (0, 70, 0, 0, 0).$$

预先设计的参数化路径如下:

$$x_{1d} = 10\cos(0.2\chi_1) - 10,$$
$$y_{1d} = -6.18\sin(0.2\chi_1),$$
$$z_{1d} = 2\chi_1,\ x_{2d} = 10\cos(0.2\chi_2) - 10,$$
$$y_{2d} = -20 - 6.18\sin(0.2\chi_2),\ z_{2d} = 2\chi_2,$$
$$x_{3d} = 10\cos(0.2\chi_3) - 10,$$
$$y_{3d} = 20 - 6.18\sin(0.2\chi_3),\ z_{3d} = 2\chi_3.$$

采用相同的控制参数,将文献[20]中的ALOS制导策略、定视距制导策略与本文所提出ALOS制导策略进行对比,仿真结果如图2～图9所示,其中定视距制导策略的前视距离分别取为1和10.

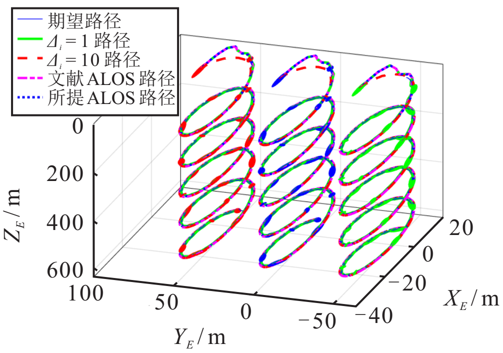

图2 路径跟踪性能对比

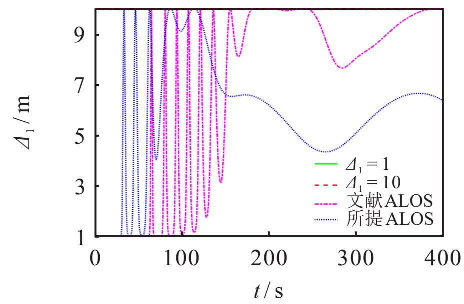

图3 前视距离对比

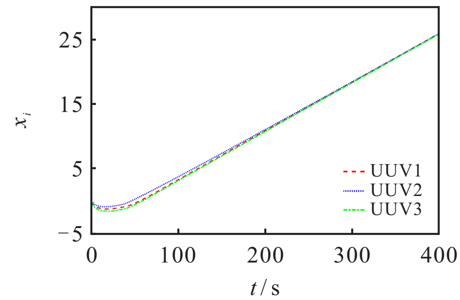

图4 路径参数χ

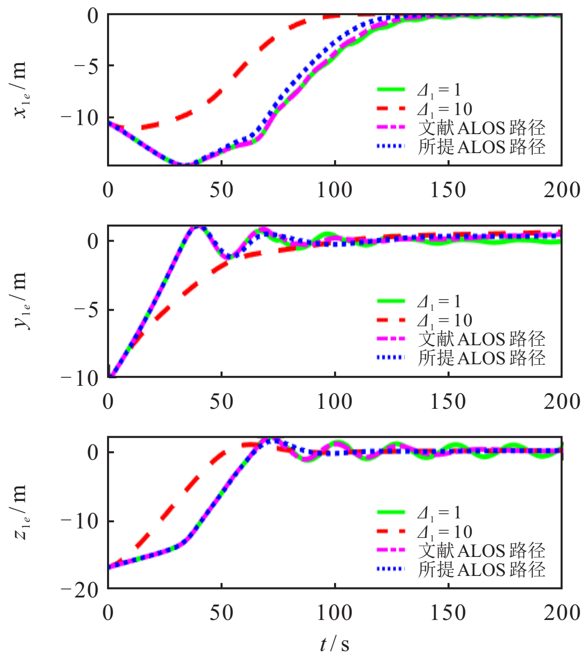

图5 路径跟踪误差对比

图2为3艘UUV在3种不同制导策略下的协同路径跟踪效果,可以看出,3种策略均可引导UUV集群协同跟踪所设计的三维参数化路径. 图3给出了3种制导策略下第1艘UUV的前视距离变化曲线,可以看出,文献ALOS和所提出ALOS均可自动调整前视距离大小,但所提出ALOS制导策略反应灵敏、震荡次数少、收敛速度快,取值更趋近于最优解. 图4给出3艘UUV的路径参数更新情况,可以看出,经过一段时间后,各UUV的路径参数趋于一致,即实现了协

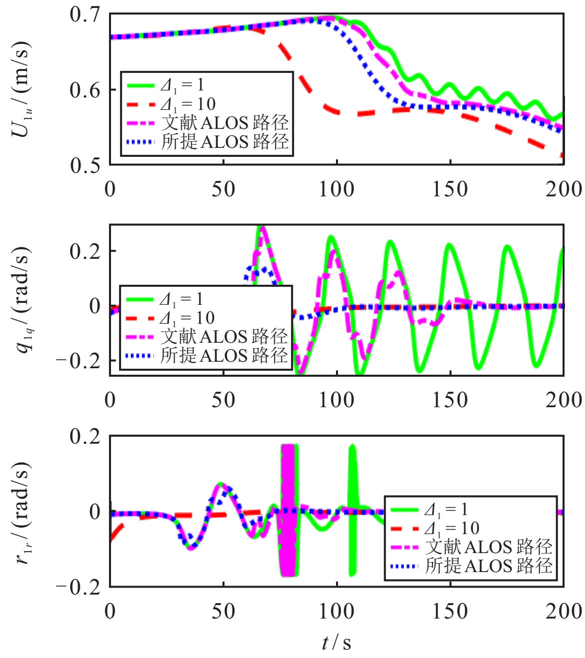

图6　制导速度对比

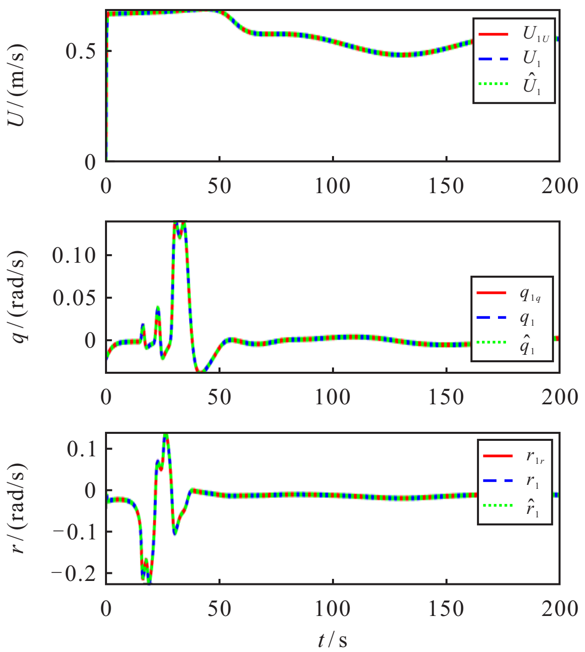

图7　速度跟踪和估计效果

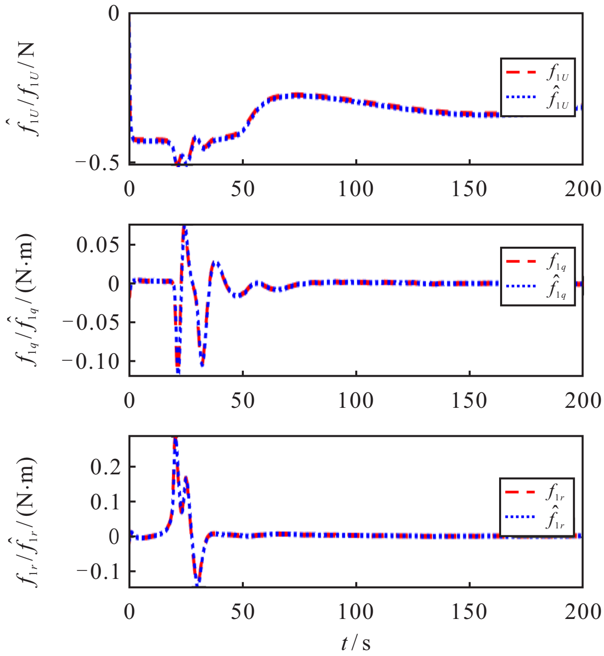

图8　动态变化模型和外部扰动估计

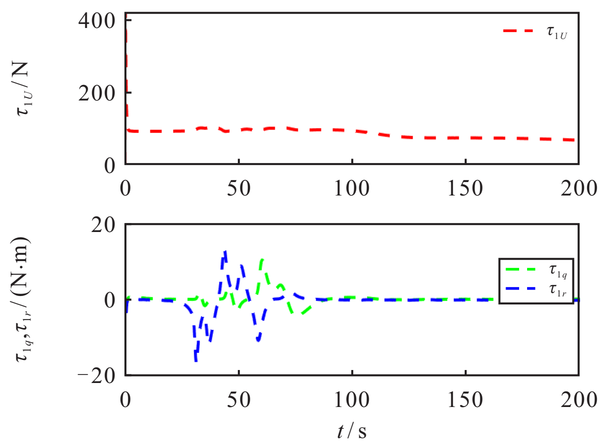

图9　控制输入

同编队控制. 图5为3种制导策略下第1艘UUV的纵向跟踪误差、横向跟踪误差和垂向跟踪误差, 由图示可知, 采用所提出ALOS制导策略的跟踪误差收敛速度更快, 收敛过程也更加平滑. 分析图6的前向制导速度与制导角速度可知, 与文献ALOS制导策略和定视距制导策略相比, 所提出ALOS制导策略对应的前向制导速度响应更加迅速, 制导角速度收敛迅速且波动较小, 具有更好的动态跟踪能力. 图7为制导速度、ESO估计速度与实际速度之间的关系, 可以看出, 所提出动力学自抗扰控制器能够控制UUV很好地跟踪制导信号, 并能有效估计UUV的实际速度. 图8描绘了ESO估计的动态变化模型和外部扰动, 可以看出, ESO能够实现二者的统一估计, 具有良好的估计性能. 图9为UUV的3个控制输入.

5　结　论

本文针对跟踪路径复杂、立体空间运动、模型参数动态变化、风浪流扰动下的UUV集群协同路径跟踪问题开展研究. 在运动学方面, 设计了自适应前视距离策略、三维ALOS制导律和协同控制律引导UUV集群在三维空间中沿参数化路径运动; 在动力学层面, 设计了自抗扰控制器实现对动态变化模型、总扰动信息和速度信息的统一估计, 有效保证了动力学控制的稳定性. 仿真结果验证了所提出基于ALOS制导的无人潜航器集群三维协同路径跟踪控制方法的有效性. 在未来的工作中, 将采用所提出方法进行UUV集群的实际航行验证.

参考文献(References)

[1] 闫敬, 陈天明, 关新平, 等. 自主水下航行器协同控制研究现状与发展趋势[J]. 水下无人系统学报, 2023, 31(1): 108-120.
(Yan J, Chen T M, Guan X P, et al. Autonomous undersea vehicle cooperative control: Current research status and development trends[J]. Journal of Unmanned Undersea Systems, 2023, 31(1): 108-120.)

[2] Yang Y, Xiao Y, Li T S. A survey of autonomous underwater vehicle formation: Performance, formation control, and communication capability[J]. IEEE Communications Surveys & Tutorials, 2021, 23(2): 815-841.

[3] Cao W Q, Yan J, Yang X, et al. Model-free formation control of autonomous underwater vehicles: A broad learning-based solution[J]. CAA Journal of Automatica Sinica, 2023, 10(5): 1325-1328.

[4] Cui R X, Sam Ge S, Voon Ee How B, et al. Leader-follower formation control of underactuated autonomous underwater vehicles[J]. Ocean Engineering, 2010, 37(17/18): 1491-1502.

[5] Yan Z P, Liu Y B, Yu C B, et al. Leader-following coordination of multiple UUVs formation under two independent topologies and time-varying delays[J]. Journal of Central South University, 2017, 24(2): 382-393.

[6] Cui R X, Yan W S, Xu D M. Synchronization of multiple autonomous underwater vehicles without velocity measurements[J]. Science China Information Sciences, 2012, 55(7): 1693-1703.

[7] Hu Z L, Ma C, Zhang L X, et al. Formation control of impulsive networked autonomous underwater vehicles under fixed and switching topologies[J]. Neurocomputing, 2015, 147: 291-298.

[8] 闫敬, 徐龙, 曹文强, 等. 基于深度强化学习的多潜器编队控制算法设计[J]. 控制与决策, 2023, 38(5): 1457-1463.
(Yan J, Xu L, Cao W Q, et al. Design of formation control algorithm for multiple autonomous underwater vehicles based on deep reinforcement learning[J]. Control and Decision, 2023, 38(5): 1457-1463.)

[9] Wang H L, Wang D, Zhang F M, et al. Self-triggered three-dimensional coordinated path following of disk-type autonomous underwater gliders based on low-frequency learning fuzzy predictors[J]. Ocean Engineering, 2021, 242: 110104.

[10] Lee J, Kim N. Backward path following using pure pursuit guidance and nonlinear guidance for UUV under strong current[J]. Journal of Ocean Engineering and Technology, 2016, 30(1): 32-43.

[11] 杨佳, 闫杰, 尉建利. 基于平行接近法的自适应滑模制导律研究[J]. 航空计算技术, 2018, 48(3): 13-16.
(Yang J, Yan J, Yu J L. Research on adaptive sliding mode guidance law based on parallel approach[J]. Aeronautical Computing Technique, 2018, 48(3): 13-16.)

[12] Fossen T I, Breivik M, Skjetne R. Line-of-sight path following of underactuated marine craft[J]. IFAC Proceedings Volumes, 2003, 36(21): 211-216.

[13] Gu N, Wang D, Peng Z H, et al. Advances in line-of-sight guidance for path following of autonomous marine vehicles: An overview[J]. IEEE Transactions on Systems, Man, and Cybernetics: Systems, 2023, 53(1): 12-28.

[14] 刘磊, 范云生, 沈心乐. 无人水面艇模糊自抗扰路径跟踪控制的研究与验证[J]. 船舶工程, 2023, 45(1): 120-128.
(Liu L, Fan Y S, Shen X L. Research and verification of fuzzy ADRC path following controller for USV[J]. Ship Engineering, 2023, 45(1): 120-128.)

[15] Børhaug E, Pavlov A, Panteley E, et al. Straight line path following for formations of underactuated marine surface vessels[J]. IEEE Transactions on Control Systems Technology, 2011, 19(3): 493-506.

[16] Wu W, Peng Z, Wang D, et al. Network-based line-of-sight path tracking of underactuated unmanned surface vehicles with experiment results[J]. IEEE Transactions on Cybernetics, 2022, 52(10): 10937-10947.

[17] 周彬, 黄兵, 毛磊, 等. 基于前视角引导的欠驱动水面无人艇自适应路径跟踪控制[J]. 哈尔滨工程大学学报, 2023, 44(1): 73-80.
(Zhou B, Huang B, Mao L, et al. Adaptive path tracking control of underactuated unmanned surface vessels based on the frontal point of view[J]. Journal of Harbin Engineering University, 2023, 44(1): 73-80.)

[18] 张伟, 郁晨曦, 滕延斌, 等. 基于模型预测控制的UUV路径跟踪控制研究[J]. 仪器仪表学报, 2017, 38(11): 2659-2666.
(Zhang W, Yu C X, Teng Y B, et al. Research on UUV path tracking control based on model predictive control[J]. Chinese Journal of Scientific Instrument, 2017, 38(11): 2659-2666.)

[19] 王晓伟, 姚绪梁, 王峰, 等. 基于滑模控制的AUV运动仿真系统[J]. 控制工程, 2017, 24(12): 2526-2533.
(Wang X W, Yao X L, Wang F, et al. An AUV motion simulation system based on sliding mode control[J]. Control Engineering of China, 2017, 24(12): 2526-2533.)

[20] 刘清河, 王泽文, 赵立军. 自适应LOS制导结合MPC控制的车辆循迹优化[J]. 哈尔滨工业大学学报, 2022,

54(1): 96-104.
(Liu Q H, Wang Z W, Zhao L J. Vehicle tracking optimization based on adaptive LOS guidance and MPC control[J]. Journal of Harbin Institute of Technology, 2022, 54(1): 96-104.)

[21] Song L F, Xu C Y, Hao L, et al. Research on PID parameter tuning and optimization based on SAC-auto for USV path following[J]. Journal of Marine Science and Engineering, 2022, 10(12): 1847.

[22] Jiang X L, Xia G H, Feng Z G, et al. Nonfragile formation seeking of unmanned surface vehicles: A sliding mode control approach[J]. IEEE Transactions on Network Science and Engineering, 2022, 9(2): 431-444.

[23] Gonzalez-Garcia A, Castaneda H. Guidance and control based on adaptive sliding mode strategy for a USV subject to uncertainties[J]. IEEE Journal of Oceanic Engineering, 2021, 46(4): 1144-1154.

[24] Gu N, Wang D, Peng Z, et al. Adaptive bounded neural network control for coordinated path-following of networked underactuated autonomous surface vehicles under time-varying state-dependent cyber-attack[J]. ISA Transactions, 2020, 104: 212-221.

[25] 李泽宇, 刘卫东, 李乐, 等. 基于RBF网络Q学习的AUV路径跟踪控制方法[J]. 西北工业大学学报, 2021, 39(3): 477-483.
(Li Z Y, Liu W D, Li L, et al. Path following method for AUV based on Q-learning and RBF neural network[J]. Journal of Northwestern Polytechnical University, 2021, 39(3): 477-483.)

[26] Makavita C D, Jayasinghe S G, Nguyen H D, et al. Experimental study of command governor adaptive control for unmanned underwater vehicles[J]. IEEE Transactions on Control Systems Technology, 2019, 27(1): 332-345.

[27] Zhang Z C, Wu Y Q. Adaptive fuzzy tracking control of autonomous underwater vehicles with output constraints[J]. IEEE Transactions on Fuzzy Systems, 2021, 29(5): 1311-1319.

[28] Fu M Y, Yu L L. Finite-time extended state observer-based distributed formation control for marine surface vehicles with input saturation and disturbances[J]. Ocean Engineering, 2018, 159: 219-227.

[29] Li M C, Guo C, Yu H M. Global finite-time control for coordinated path following of multiple underactuated unmanned surface vehicles along one curve under directed topologies[J]. Ocean Engineering, 2021, 237: 109608.

[30] Xue W C, Chen S, Zhao C, et al. On integrating uncertainty estimator into PI control for a class of nonlinear uncertain systems[J]. IEEE Transactions on Automatic Control, 2021, 66(7): 3409-3416.

[31] 王浩亮, 柴亚星, 王丹, 等. 基于事件触发机制的多自主水下航行器协同路径跟踪控制[J]. 自动化学报, 2024, 50(5): 1024-1034.
(Wang H L, Chai Y X, Wang D, et al. Event-triggered cooperative path following of multiple autonomous underwater vehicles[J]. Acta Automatica Sinica, 2024, 50(5): 1024-1034.)

[32] Pettersen K Y, Egeland O. Time-varying exponential stabilization of the position and attitude of an underactuated autonomous underwater vehicle[J]. IEEE Transactions on Automatic Control, 1999, 44(1): 112-115.

[33] Ceragioli F, De Persis C, Frasca P. Discontinuities and hysteresis in quantized average consensus[J]. Automatica, 2011, 47(9): 1916-1928.

[34] Krstić M, Kanellakopoulos I, Kokotović P V. Nonlinear and adaptive control design[M]. New York: Wiley, 1995: 501-507.

作者简介

王浩亮 (1985−), 男, 教授, 博士, 主要研究方向为海洋无人航行器规划、控制与协同, E-mail: haoliang.wang12@dlmu.edu.cn;

于德智 (2000−), 男, 硕士生, 主要研究方向为海洋无人航行器协同控制, E-mail: 15845626195@163.com;

卢丽宇 (1998−), 男, 博士生, 主要研究方向为多无人船集群控制, E-mail: lly1131@126.com;

张卫东 (1967−), 男, 教授, 博士, 主要研究方向为智能控制理论和人工智能理论, E-mail: wdzhang@sjtu.edu.cn;

彭周华 (1982−), 男, 教授, 博士, 主要研究方向为多无人船集群控制, E-mail: zhpeng@dlmu.edu.cn.